

Extensions of Johnson's Theory of Backward-Wave Oscillations in a Traveling-Wave Tube

Abhijit Jassem^{ID}, Patrick Y. Wong^{ID}, David P. Chernin^{ID}, Y. Y. Lau^{ID}, Fellow, IEEE, Foivos Antoulinakis, Drew Packard^{ID}, Thomas A. Hargreaves^{ID}, and Carter M. Armstrong^{ID}

Abstract—This paper extends Johnson's classical theory [Johnson, Proc. IRE 43, 684 (1955)] for the threshold of backward-wave oscillation (BWO) in a traveling-wave tube by considering the effects of: 1) small random variations of the circuit phase velocity along the tube axis and 2) end reflections. We find that both the BWO threshold and BWO frequency are minimally affected by random variations of the phase velocity, but we find that the oscillation threshold depends sensitively on the magnitude and phase of the composite reflection coefficients.

Index Terms—Backward-wave oscillations (BWOs), random variations, traveling-wave tubes (TWTs).

I. INTRODUCTION

BACKWARD-WAVE oscillations (BWOs) pose a serious threat to the stability of a traveling-wave tube (TWT) [1]–[7]. These oscillations occur near the intersection of the forward-propagating beam mode and the backward-wave mode of the slow-wave structure in the (ω, β) dispersion diagram, where ω is the frequency and β is the propagation constant. These backward-wave modes have a forward (positive) phase velocity and a backward (negative) group velocity. BWO is different from regenerative oscillations, which are caused by reflection and reamplification of an in-band signal that co-propagates with the electron beam. It is also different from the band edge oscillations [8]–[10], which occur near a zero group velocity point of the dispersion diagram for the slow-wave structure.

Johnson developed the classical theory for the onset of BWO in a TWT [1], [2] for a uniform circuit in the absence of end reflections. His threshold condition for BWO is given in terms of the starting length L at a given current. This

Manuscript received September 14, 2018; revised December 22, 2018; accepted December 28, 2018. Date of publication January 31, 2019; date of current version February 22, 2019. This work was supported in part by Leidos, Inc. through DARPA under Contract HR0011-16-C-0080, in part by AFOSR under Grant FA9550-15-1-0097 and Grant FA9550-14-1-0309, and in part by the L3 Technologies Electron Devices Division. The review of this paper was arranged by Editor M. Thumm. (*Corresponding author: Y. Y. Lau*)

A. Jassem, P. Y. Wong, Y. Y. Lau, F. Antoulinakis, and D. Packard are with the Department of Nuclear Engineering and Radiological Sciences, University of Michigan, Ann Arbor, MI 48109 USA (e-mail: yylau@umich.edu).

D. P. Chernin is with Leidos Corporation, Reston, VA 20190 USA.

T. A. Hargreaves and C. M. Armstrong are with L3 Technologies, Torrance, CA 90505 USA.

Color versions of one or more of the figures in this paper are available online at <http://ieeexplore.ieee.org>.

Digital Object Identifier 10.1109/TED.2019.2893574

starting length, together with the frequency of BWO, must be obtained numerically from a transcendental relation, (see Section II). An interesting feature of Johnson's theory is that his threshold condition depends only on the two Pierce parameters, QC and d , where QC is the so-called space charge parameter, and d measures the cold-tube loss, both evaluated at the BWO frequency [1], [2]. Johnson [1] reported that his theory yielded good agreement with the experimental observations. However, we would point out that it remains an open question on how to determine QC accurately for a realistic slow-wave structure [11]–[13].

In this paper, we consider the effects of random axial variations of the circuit phase velocity on Johnson's threshold conditions. We find that these random variations only minimally affect the threshold conditions. We next remove the random variation of the phase velocity, but take into account the end reflections by including the forward propagating circuit mode, which is at the same frequency of BWO, but does not interact with the beam. We find that the resulting threshold conditions depend sensitively on the amplitude and phase of the composite reflection coefficient.

Our treatment of the starting condition for BWO generally follows Johnson's approach, which is very different from that of Levush *et al.* [5], who also considered BWO in a TWT including the effects of end reflections. It is difficult to compare this paper and that of Johnson to that of Levush *et al.* [5] since the latter authors did not formulate their theory in terms of Pierce parameters, and therefore did not show the explicit dependence of the threshold on QC and d as in Johnson's theory. In fact, Levush *et al.* [5] assume that the cold-tube circuit is lossless; so they cannot be readily used to compare with BWO experiments which exhibit cold-tube loss. Moreover, the threshold oscillation condition in [5] depends explicitly on the group velocity of the backward circuit mode, while the group velocity (and the backward-wave signal propagation time) does not enter explicitly in Johnson's theory. We have been consequently unable to determine the precise relation between the approach and results of Levush *et al.* [5] and those of Johnson [1]. Other references on BWO in a TWT may be found in [14]–[20].

This paper was in part motivated by a test experimental helix TWT built by L3 Technologies, dedicated to the study of BWO excitation. In that experiment, BWO was not observed even though it was predicted to occur according to the classical Johnson theory. The extension of Johnson's theory given here was insufficient to explain why this tube did not oscillate.



Fig. 1. Example of random variations along the tube axis; b is Pierce's detune parameter.

A preliminary report of this experiment was presented in a conference abstract [21].

II. EFFECTS OF RANDOM VARIATIONS IN PHASE VELOCITY

For a uniform tube, the incremental complex wavenumbers, δ_1 , δ_2 , and δ_3 satisfy Pierce's three-wave dispersion relation for the backward wave with $e^{j\omega t - j\beta z}$ dependence [1], [2]

$$(\delta^2 + 4QC)(\delta + jb - d) = j \quad (1)$$

where $\delta = -j(\beta - \beta_e)/C\beta_e$ and $b = (v_0/v_p - 1)/C$ is the mismatch between the beam velocity v_0 and the phase velocity of the backward wave v_p , $\beta_e = \omega/v_0$ is the propagation constant of the beam mode, C is Pierce's dimensionless gain parameter, and QC is Pierce's space charge parameter, all referring to the backward-wave mode [1].¹ When the circuit parameters v_p , C , or d are allowed to vary axially, as shown in Fig. 1, (1) is no longer applicable, and these three waves are governed by the nondimensional differential equation [6], [22], [23]

$$\frac{d^3 f(x)}{dx^3} + jC(b + jd) \frac{d^2 f(x)}{dx^2} + C^2(4QC) \frac{df(x)}{dx} + jC^3(4QC(b + jd) - 1)f(x) = 0 \quad (2)$$

where $x = \beta_e z$ is the normalized axial distance, $f(x) = e^{jx}s(x)$, and $s(x)$ is the small signal displacement of an electron from its unperturbed orbit. In terms of f , the circuit wave RF electric field, $a(x)$, evolves according to

$$\frac{a(0)}{a(x)} = \frac{f''(0) + 4QC^3 f(0)}{f''(x) + 4QC^3 f(x)} = \frac{1}{f''(x) + 4QC^3 f(x)} \quad (3)$$

where we have used the “initial” conditions to (2)

$$f(0) = 0, \quad f'(0) = 0, \quad f''(0) = 1 \quad (4)$$

which represent, respectively, zero ac current, zero ac velocity, and unit output electric field [6], [22], [23], [24] in the present linear theory. For the backward-wave amplification, the input is located downstream, at $z = L$ (Fig. 1).

For a uniform tube, one finds from (2) to (4)

$$\begin{aligned} \frac{a(\beta_e L)}{a(0)} e^{j2\pi N} &= \frac{\delta_1^2 + 4QC}{(\delta_1 - \delta_2)(\delta_1 - \delta_3)} e^{2\pi\delta_1 CN} \\ &+ \frac{\delta_2^2 + 4QC}{(\delta_2 - \delta_3)(\delta_2 - \delta_1)} e^{2\pi\delta_2 CN} \\ &+ \frac{\delta_3^2 + 4QC}{(\delta_3 - \delta_1)(\delta_3 - \delta_2)} e^{2\pi\delta_3 CN} \end{aligned} \quad (5)$$

¹See Eqs. (11.1-11), (11.1-9), and (11.2-7) of Ref. [2].

which is [2, eq. (11.1-15)]. Here, $N = \beta_e L/2\pi$ is the length of tube, measured in the number of axial wavelengths of the beam mode, and δ_1 , δ_2 , and δ_3 are the three roots of the three-wave dispersion relation, (1). In Johnson's theory, it is assumed that QC and d are given. The values of CN (starting length or threshold current) and b (BWO oscillation frequency) are then determined numerically so that the real and imaginary parts of RHS of (5) are both equal to 0. Thus, the threshold current and the oscillation frequency of BWO, according to Johnson's theory, depend only on the secondary parameters, QC and d . For QC = 0 and $d = 0$, Johnson found CN = 0.314 and $b = 1.522$. For nonzero values of QC and b , the values of CN and b are tabulated [1], [2]. Johnson claimed that his threshold condition gave good agreement with experiments, but there was insufficient information for us to validate such claims, as the values of QC and d are largely unknown for the experiments.

Random variations in the phase velocity affect the gain the most [6], [22], [23], so we consider only this aspect in this section. We assume that there is a random variation only in Pierce's detune parameter b , while all other parameters C , QC, and d are assumed to be constants in (2). We set $b(x) = b_0 + b_1(x)$ where b_0 is the constant mean value, and $b_1(x)$ is the perturbative quantity that is obtained by linearly interpolating between randomly generated neighboring “nodes,” as shown in Fig. 1 [6], [22], [23]. We set $x = \beta_e L = 100$, and the value of b_1 at $x = 1, 2, 3, \dots, 100$ is set by an independent Gaussian random number generator with a specified standard deviation σ_b . The standard deviation in the circuit phase velocity σ_q , where $q = (v_p - v_{p0})/v_{p0}$, is approximately related to σ_b , by $\sigma_b = (\sigma_q/C)(1 + Cb_0)$ [22]. The piecewise linear function shown in Fig. 1 serves as one “case” that simulates a TWT with random variations in the phase velocity. To obtain good statistics, 1000 such cases were generated, each of which was applied to (2).

To extract the threshold BWO conditions, we have to determine the values of b_0 and C that solve the third-order differential equation, (2), subject to the initial conditions (4), which yield a zero normalized circuit electric field at $z = L$. This was done by the use of the unconstrained optimization algorithm “fminsearch” in MATLAB, which uses the Nelder-Mead simplex algorithm described in Lagarias *et al.* [25]. For each random sample $b_1(x)$, an initial guess at the value of b_0 and C is provided by the pristine tube solution. The optimization algorithm is then run; this essentially guesses the values of b_0 and C , solves (2) for each guess, then tries to find the guess that minimizes the value of $f''(x) + C^2(4QC)f(x)$ at $x = 100$, see (3). To validate this approach, an error-free case was run with QC = 0 and $d = 0$ with an arbitrary initial guess; this resulted in values of $b = 1.522$ and $C = 0.0197$. Since $x = \beta_e L = 100$, $N = 100/2\pi = 15.92 \Rightarrow CN = (0.0197)(15.92) = 0.314$. These values match the published results of Johnson under the same conditions of QC = 0 and $d = 0$ [1], [2].

The statistical distribution of the threshold value of Pierce's gain parameter C for the onset of BWO is shown in Fig. 2 for these 1000 cases, setting $d = 0$ and QC = 0. Here, we see that the BWO threshold for C_0 [Fig. 2(a)] was only minimally affected by the random variations in the phase velocity.

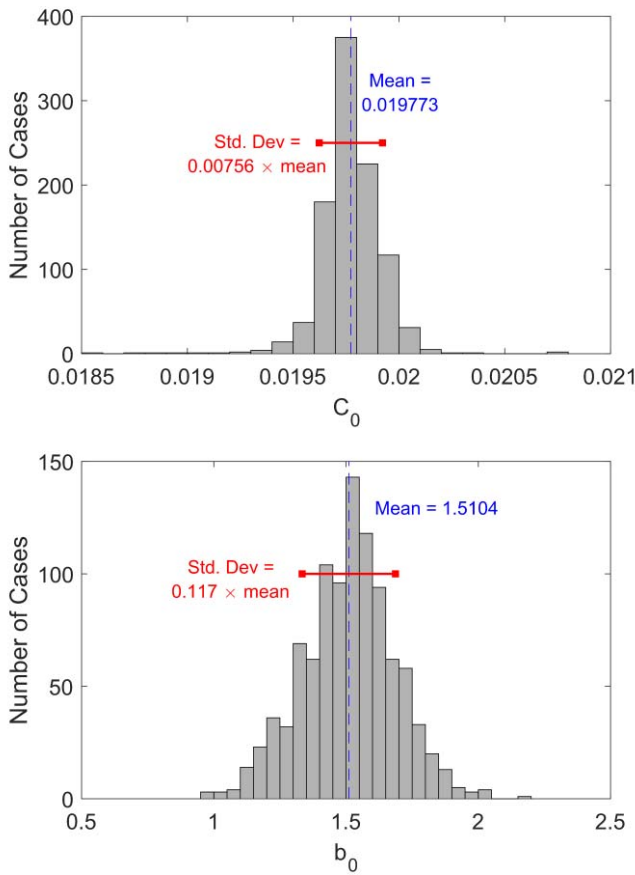


Fig. 2. Distribution in threshold for $QC = 0$ and $d = 0$ cases. (a) Pierce gain parameter C (top) and (b) detune parameter b for variation in detune parameter $\sigma_b = 1.7$ (bottom) (corresponding to the standard deviation in circuit phase velocity of 3.4%).

This relative insensitivity of Johnson's BWO threshold is likely due to the cancelation of all the three waves at $z = L$ (Fig. 1), and therefore, the sensitivity of b that characterizes synchronous interaction is of lesser importance. The large spread in b_0 shown in Fig. 2(b) was self-imposed as we assumed $\sigma_b = 1.7$. The corresponding spread in the BWO frequency is $C\sigma_b = 3.4\%$ since $C = 0.02$ from Fig. 2(a). The spread in the threshold current, i.e., in C^3 , is also of order 3.4% (not shown). The effect of nonzero QC is shown in Fig. 3, which shows that the value of the threshold C increases by 50% as QC increases from 0 to 1. Fig. 3 shows that the mean values of threshold C and b are very close to those in an error-free tube, and that for $QC > 0.25$, to a good approximation, $b_{\text{thres}} \cong \sqrt{4QC}$ and $C_{\text{thres}} \cong ((QC)^{(1/4)})/2N$, as established by Johnson [1], see [2, pp. 407].

III. EFFECTS OF END REFLECTIONS

To consider the effects of end reflections on Johnson's BWO thresholds, we add the forward wave a_f of the circuit electric field to the backward wave a_b of the circuit electric field, as shown in Fig. 4. Note that a_b was denoted by a in (3) and (5). To simplify the analysis, in this section, we suppress the axial variations in all the Pierce parameters. At the BWO oscillation frequency, the forward circuit wave hardly interacts with the electron beam, so we assume that it has a constant amplitude between $z = 0$ and $z = L$, while the

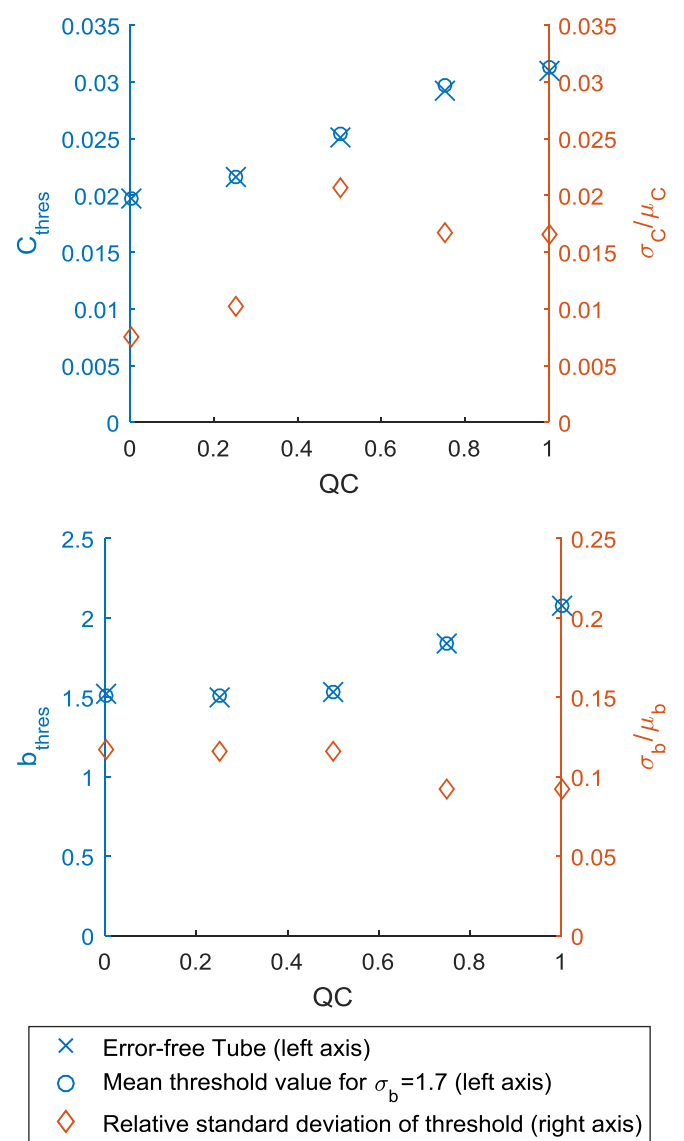


Fig. 3. (a) Means and relative standard deviations of gain parameter C and (b) detune parameter b as a function of QC.

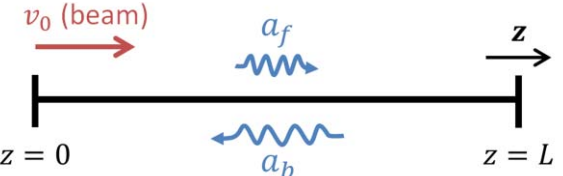


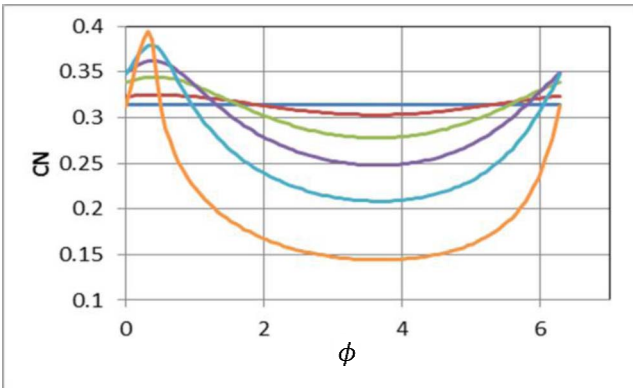
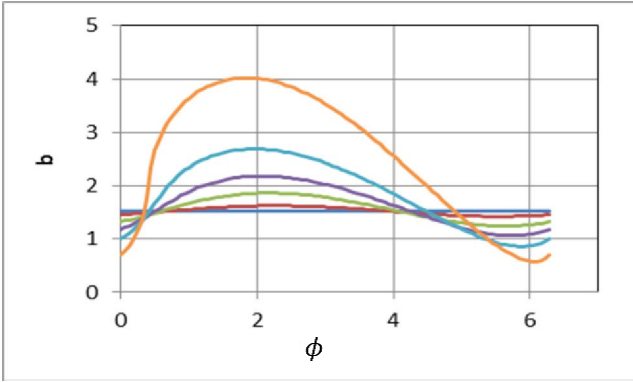
Fig. 4. Forward and backward waves for the end reflection model.

backward-wave circuit electric field a_b could vary with z in general. Thus, we write

$$a_f = \tilde{a}_f \exp(j\omega t - jk_f z) \quad (6)$$

$$a_b = \tilde{a}_b(z) \exp(j\omega t) \quad (7)$$

where \tilde{a}_f is a constant and k_f is the wavenumber of the forward propagating circuit mode, assuming no attenuation in this forward wave. The forward circuit wave has no gain since the beam's velocity is very different from the phase velocity of this forward wave at the BWO frequency. We next define the reflection coefficients R_0 and R_L , at $z = 0$ and at $z = L$,



— R=0 — R=0.1 — R=0.3
— R=0.5 — R=0.7 — R=0.9

Fig. 5. Effect of end reflections on the threshold BWO conditions for (a) b (top) and (b) CN for $QC = 0$ and $d = 0$ cases (bottom).

respectively, as

$$\begin{aligned} R_0 &\equiv \frac{a_f(z=0)}{a_b(z=0)} \\ R_L &\equiv \frac{a_b(z=L)}{a_f(z=L)}. \end{aligned} \quad (8)$$

Multiplying the two equations in (8), we construct a composite reflection coefficient R with an associated phase θ as follows:

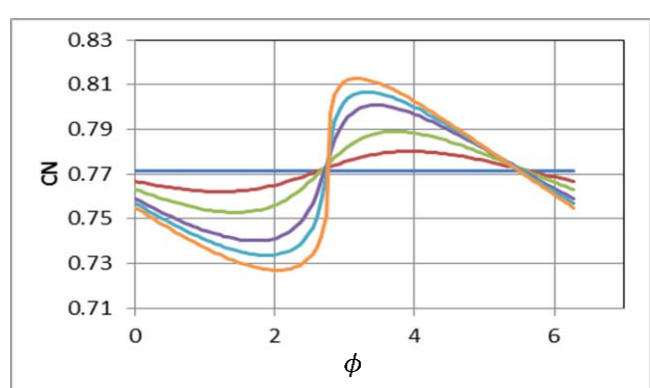
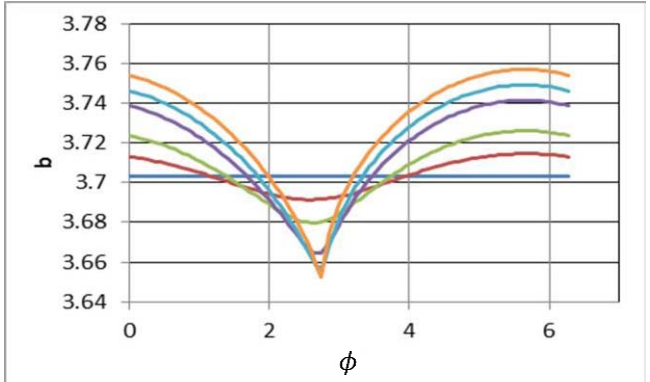
$$\frac{a_b(z=L)}{a_b(z=0)} = R_L R_0 \frac{a_f(z=L)}{a_f(z=0)} = R_L R_0 e^{-j k_f L} \equiv R e^{j \theta} \quad (9)$$

where we have used (6) and defined $R = |R_0 R_L|$. Inclusion of attenuation in the forward wave in (6) would only change the composite reflection coefficient R .

The effects of end reflections on the BWO threshold condition may be obtained by inserting (9) into (5), which is now modified to read

$$\begin{aligned} \frac{\delta_1^2 + 4QC}{(\delta_1 - \delta_2)(\delta_1 - \delta_3)} e^{2\pi\delta_1 CN} + \frac{\delta_2^2 + 4QC}{(\delta_2 - \delta_3)(\delta_2 - \delta_1)} e^{2\pi\delta_2 CN} \\ + \frac{\delta_3^2 + 4QC}{(\delta_3 - \delta_1)(\delta_3 - \delta_2)} e^{2\pi\delta_3 CN} = R e^{j\phi} \quad (10) \end{aligned}$$

where $\phi = \theta + 2\pi N$. If $R = 0$, (10) reduces to Johnson's BWO threshold condition [1], [2]. This is the case when the



— R=0 — R=0.03 — R=0.06
— R=0.1 — R=0.12 — R=0.14

Fig. 6. Effect of end reflections on the threshold BWO conditions for (a) b (top) and (b) CN for $QC = 3.392$ and $d = 0.135$ cases (L3 TWT [21]) (bottom).

slow-wave TWT circuit is perfectly matched at either terminations, at $z = 0$ or at $z = L$, hence $R = 0$.

We then use an interior-point algorithm [26] with the “fmincon” MATLAB optimization function to find the threshold values of b and CN that satisfy (1) and (10) in the zero space charge and zero circuit loss ($QC = 0$ and $d = 0$) case for a range of $R \in [0, 1]$ and $\phi \in [0, 2\pi]$. These solutions, given in Fig. 5, show that end reflections can have a significant impact on the threshold conditions depending on the magnitude of the reflection coefficient. From Fig. 5(b), one can claim that end reflections tend to decrease the required starting current, a result largely consistent with Levush *et al.* [5], whose formulation is very different from Johnson [1]. The threshold conditions, for example, with nonzero values of QC and d are presented in Fig. 6 for values of R up to 0.14. However, at higher reflection coefficients ($R > 0.14$), the transcendental equation, (10), does not have a meaningful solution, similar to the case of N which satisfies $A = \cos(2\pi N)$ when $A > 1$. When no threshold condition can be found, this means that BWO does not exist for the set of parameters QC , d , R , and ϕ .

IV. CONCLUSION

This paper reveals that the effects of random manufacturing errors along TWT only minimally affect Johnson's threshold for the starting length, as measured by CN, for the onset

of BWO. The BWO oscillation frequency and the threshold current (at a fixed circuit length) were found to be affected to a similar degree as the variation in the circuit phase velocity. This insensitivity is quite different from some previous works where large gain ripples in a forward-wave TWT may result from random variations of b along the tube [7], in part due to our neglect of internal reflections that were carefully accounted for in [7], and in part due to Johnson's threshold arising from the cancelation of the three waves at $z = L$, thereby reducing the sensitivity to b . Next, we considered an error-free tube but included the effects of reflections of the circuit wave on the tube ends in Johnson's BWO theory. We found that in the zero space charge, zero cold circuit loss case, the required starting current for the onset of oscillation was on average decreased as a result of these reflections.

Our generalization of Johnson's theory did not explain why an L3 helix TWT [21] did not oscillate even though the Pierce parameter CN in the experiment exceeded the theoretical threshold value. One reason, we suspect, is that the values of QC, d , the reflection coefficients, and/or the beam radius required for application of Johnson's theory may not be known with sufficient accuracy.

ACKNOWLEDGMENT

The views, opinions, and/or findings expressed are those of the authors and should not be interpreted as representing the official views or policies of the Department of Defense or the U.S. Government. Approved for Public Release, Distribution Unlimited.

REFERENCES

- [1] H. R. Johnson, "Backward-wave oscillators," *Proc. IRE*, vol. 43, no. 6, pp. 684–697, Jun. 1955, doi: [10.1109/JRPROC.1955.278054](https://doi.org/10.1109/JRPROC.1955.278054).
- [2] J. W. Gewartowski and H. A. Watson, *Principles of Electron Tubes: Including Grid-Controlled Tubes, Microwave Tubes and Gas Tubes*. New York, NY, USA: Van Nostrand, 1965.
- [3] A. S. Gilmour, *Principles of Traveling Wave Tubes*. Norwood, MA, USA: Artech House, 1994.
- [4] J. R. Pierce, *Traveling-Wave Tubes*. New York, NY, USA: Van Nostrand, 1950.
- [5] B. Levush, T. M. Antonsen, A. Bromborsky, W.-R. Lou, and Y. Carmel, "Theory of relativistic backward-wave oscillators with end reflectors," *IEEE Trans. Plasma Sci.*, vol. 20, no. 3, pp. 263–280, Jun. 1992, doi: [10.1109/27.142828](https://doi.org/10.1109/27.142828).
- [6] S. Sengle, M. L. Barsanti, T. A. Hargreaves, C. M. Armstrong, J. H. Booske, and Y. Y. Lau, "Impact of random fabrication errors on backward-wave small-signal gain in traveling wave tubes with finite space charge electron beams," *J. Appl. Phys.*, vol. 113, no. 7, p. 074905, Feb. 2013, doi: [10.1063/1.4792666](https://doi.org/10.1063/1.4792666).
- [7] D. Chernin, I. Rittersdorf, Y. Y. Lau, T. M. Antonsen, and B. Levush, "Effects of multiple internal reflections on the small-signal gain and phase of a TWT," *IEEE Trans. Electron Devices*, vol. 59, no. 5, pp. 1542–1550, May 2012, doi: [10.1109/TED.2012.2186141](https://doi.org/10.1109/TED.2012.2186141).
- [8] A. P. Kuznetsov, S. P. Kuznetsov, A. G. Rozhnev, E. V. Blokhina, and L. V. Bulgakova, "Wave theory of a traveling-wave tube operated near the cutoff," *Radiophys. Quantum Electron.*, vol. 47, no. 5, pp. 356–373, 2004, doi: [10.1023/B:RAQE.0000046310.29763.c1](https://doi.org/10.1023/B:RAQE.0000046310.29763.c1).
- [9] D. M. H. Hung *et al.*, "Absolute instability near the band edge of traveling-wave amplifiers," *Phys. Rev. Lett.*, vol. 115, no. 12, p. 124801, Sep. 2015, doi: [10.1103/PhysRevLett.115.124801](https://doi.org/10.1103/PhysRevLett.115.124801).
- [10] F. Antoulakis, P. Wong, A. Jassem, and Y. Y. Lau, "Absolute instability and transient growth near the band edges of a traveling wave tube," *Phys. Plasmas*, vol. 25, no. 7, p. 072102, Jul. 2018, doi: [10.1063/1.5028385](https://doi.org/10.1063/1.5028385).
- [11] Y. Y. Lau and D. Chernin, "A review of the AC space-charge effect in electron-circuit interactions," *Phys. Fluids B Plasma Phys.*, vol. 4, no. 11, pp. 3473–3497, Nov. 1992, doi: [10.1063/1.860356](https://doi.org/10.1063/1.860356).
- [12] D. Simon *et al.*, "On the evaluation of pierce parameters C and Q in a traveling wave tube," *Phys. Plasmas*, vol. 24, no. 3, p. 033114, 2017, doi: [10.1063/1.4978474](https://doi.org/10.1063/1.4978474).
- [13] P. Y. Wong, D. Chernin, and Y. Y. Lau, "Modification of Pierce's classical theory of traveling-wave tubes," *IEEE Electron Device Lett.*, vol. 39, no. 8, pp. 1238–1241, Aug. 2018, doi: [10.1109/LED.2018.2851544](https://doi.org/10.1109/LED.2018.2851544).
- [14] R. G. Carter, *Microwave and RF Vacuum Electronic Power Sources*. Cambridge, U.K.: Cambridge Univ. Press, 2018.
- [15] J. L. Zhang, Y. H. Lu, and J. S. Yang, "Backward-wave suppression for broadband helix traveling-wave tubes using the phase velocity variation of output circuit," *IEEE Trans. Electron Devices*, vol. 59, no. 8, pp. 2263–2267, Aug. 2012.
- [16] S. K. Datta, L. Kumar, and B. N. Basu, "A simple closed-form formula for backward-wave start-oscillation condition for millimeter-wave helix TWTs," *Int. J. Infr. Millim. Waves*, vol. 29, no. 6, pp. 608–616, 2008.
- [17] Z. Duan, Y. Gong, W. Wang, Y. Wei, and M. Huang, "Effect of attenuation on backward-wave oscillation start oscillation condition," *IEEE Trans. Plasma Sci.*, vol. 32, no. 6, pp. 2184–2188, Dec. 2004.
- [18] S. Liu, "A fast computation of the start-oscillation current of backward wave in MMW HTWT's," *Int. J. Infr. Millim. Waves*, vol. 20, no. 5, pp. 859–865, 1999.
- [19] Y. N. Pchelnikov and A. A. Elizarov, "Analysis of the methods to increase the output power and frequency of the broadband TWTs," *J. Commun. Technol. Electron.*, vol. 54, no. 9, pp. 1027–1034, 2009.
- [20] E. D. Belyavskiy, I. A. Goncharov, A. E. Martynyuk, V. A. Svirid, and S. N. Khotiantsev, "Two-dimensional small signal analysis of backward-wave oscillation in a helix traveling-wave tube under Brillouin-flow, periodic permanent magnetic focusing," *IEEE Trans. Electron Device*, vol. 48, no. 8, pp. 1727–1736, Aug. 2001, doi: [10.1109/16.936695](https://doi.org/10.1109/16.936695).
- [21] A. Jassem *et al.*, "On Johnson's backward wave oscillation thresholds in TWT," in *Proc. IEEE Int. Vac. Electron. Conf. (IVEC)*, Monterey, CA, USA, Apr. 2018, pp. 171–172, doi: [10.1109/IVEC.2018.8391479](https://doi.org/10.1109/IVEC.2018.8391479).
- [22] P. Pengvanich, D. Chernin, Y. Y. Lau, J. W. Luginsland, and R. M. Gilgenbach, "Effect of random circuit fabrication errors on small-signal gain and phase in traveling-wave tubes," *IEEE Trans. Electron Devices*, vol. 55, no. 3, pp. 916–924, Mar. 2008, doi: [10.1109/TED.2007.914840](https://doi.org/10.1109/TED.2007.914840).
- [23] I. M. Rittersdorf, T. M. Antonsen, D. Chernin, and Y. Y. Lau, "Effects of random circuit fabrication errors on the mean and standard deviation of small signal gain and phase of a traveling wave tube," *IEEE J. Electron Devices Soc.*, vol. 1, no. 5, pp. 117–128, May 2013, doi: [10.1109/JEDS.2013.2273794](https://doi.org/10.1109/JEDS.2013.2273794).
- [24] C. F. Dong *et al.*, "Harmonic content in the beam current in a traveling-wave tube," *IEEE Trans. Electron Devices*, vol. 62, no. 12, pp. 4285–4292, Dec. 2015, doi: [10.1109/TED.2015.2490584](https://doi.org/10.1109/TED.2015.2490584).
- [25] J. C. Lagarias, J. A. Reeds, M. H. Wright, and P. E. Wright, "Convergence properties of the Nelder-Mead simplex method in low dimensions," *SIAM J. Optim.*, vol. 9, no. 1, pp. 112–147, 1998, doi: [10.1137/S1052623496303470](https://doi.org/10.1137/S1052623496303470).
- [26] R. H. Byrd, M. E. Hribar, and J. Nocedal, "An interior point algorithm for large-scale nonlinear programming," *SIAM J. Optim.*, vol. 9, no. 4, pp. 877–900, 1999, doi: [10.1137/S1052623497325107](https://doi.org/10.1137/S1052623497325107).
- [27] G. M. Branch and T. G. Mihran, "Plasma frequency reduction factors in electron beams," *IRE Trans. Electron Devices*, vol. 2, no. 2, pp. 3–11, Apr. 1955, doi: [10.1109/T-ED.1955.14065](https://doi.org/10.1109/T-ED.1955.14065).



Abhijit Jassem received the B.S. degree in nuclear engineering from Purdue University, West Lafayette, IN, USA, in 2016. He is currently pursuing the Ph.D. degree with the University of Michigan's Nuclear Engineering & Radiological Sciences Program.

He is working with the Plasma, Pulsed Power, and Microwave Laboratory, University of Michigan, under the supervision of Prof. Y. Y. Lau.

Patrick Y. Wong, photograph and biography not available at the time of publication.

David P. Chernin, photograph and biography not available at the time of publication.



Y. Y. Lau (F'08) received the S.B., S.M., and Ph.D. degrees in EE from the Massachusetts Institute of Technology, Cambridge, MA, USA.

He is currently a Professor with the University of Michigan, Ann Arbor, MI, USA, specialized in RF sources, heating, and discharge.

Dr. Lau received the 1999 IEEE Plasma Science and Applications Award, and the 2017 IEEE John R. Pierce Award for Excellence in Vacuum Electronics.



Drew Packard received the B.S.E. and M.S.E. degrees in nuclear engineering and radiological sciences from the University of Michigan, Ann Arbor, MI, USA, in 2016 and 2017, respectively, where he is currently a Graduate Student with the Plasma, Pulsed Power, and Microwave Laboratory, performing research on high-power microwave devices for Prof. R. Gilgenbach.

Foivos Antoulidakis, photograph and biography not available at the time of publication.

Thomas A. Hargreaves, photograph and biography not available at the time of publication.

Carter M. Armstrong, photograph and biography not available at the time of publication.